ACS APPLIED MATERIALS & INTERFACES

Research Article

www.acsami.org

Highly Conductive One-Dimensional Nanofibers: Silvered Electrospun Silica Nanofibers via Poly(dopamine) Functionalization

Ye Fu,[†,§] Li Liu,[‡,§] Liqun Zhang,[†,‡] and Wencai Wang*[,†,‡]

[†]State Key Laboratory of Organic Inorganic Composites, Beijing 100029, China

[‡]Key Laboratory of Beijing City on Preparation and Processing of Novel Polymer Materials, Beijing 100029, China

[§]Key Laboratory of Carbon Fiber and Functional Polymers, Ministry of Education, Beijing University of Chemical Technology, Beijing 100029, China

ABSTRACT: Using tetraethyl orthosilicate as a main raw material, silica nanofibers (SiNFs) were prepared through the combination of a sol−gel process and an electrospinning technique followed by pyrolysis. Surface modified electrospun SiNFs developed by self-polymerization of polydopamine on the surface (SiNFs-PDA) served as templates for the electroless plating of silver nanoparticles (Ag NPs), using glucose as a reducing agent. The electrical resistivity of silver coated SiNPs-PDA (SiNFs-PDA/Ag) was measured by the four-point probe method and was found to be as low as 0.02 mΩ·cm at room temperature. The morphology of SiNFs-PDA/Ag before and after the blending with silicon rubber indicated a strong interaction between the silver layer and the SiNFs-PDA. The electrical and mechanical properties of the silicon rubber filled with SiNFs-PDA/Ag were studied to demonstrate the conductive performance application of SiNFs-PDA/Ag.

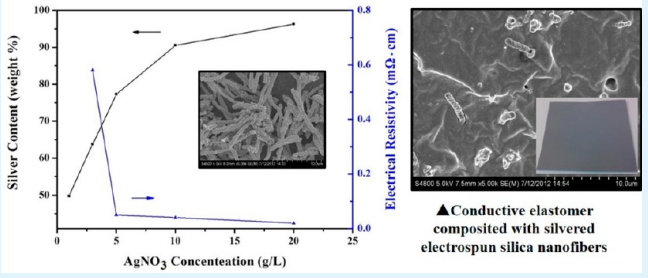

KEYWORDS: *electrospinning, silica, dopamine, silver, electrical conductivity*

1. INTRODUCTION

Composite nanostructures with nanoparticles assembled on one-dimensional substrates exhibit the unique physical and chemical properties of the core and shell materials.[1−5] Electrospinning technology has provided an innovative method for the straightforward manufacturing of continuous one-dimensional nanomaterials with controllable diameters.[6,7] Electrospun silica nanofibers (SiNFs) could be developed through the combination of a sol−gel process and an electrospinning technique, followed by pyrolysis.[8−11] As silver nanoparticles (Ag NPs) exhibit rich optical,[12−14] antimicrobial,[15,16] electronic,[17−19] and magnetic[20,21] properties, they provide an approach to make smart functional composites by depositing Ag NPs on various substrates, which perform potential applications ranging from antibacterial materials to conductive composites. In particular, these Ag NPs deposited substrates can be used as the fillers for conductive composites,[22−24] offering an application of electromagnetic interference (EMI) shielding. Zhang et al. assembled presynthesized noble nanoparticles on mesostructured silica nanofibers synthesized with a structure-directing agent through the surface functionalization of silanol.[12] Zhang et al. assembled Ag NPs on the inner and outer surfaces of electrospun silica nanotubes through the in situ reduction of Ag^{+} by Sn^{2+} ions.[25,26] However, the complicated preparation process and harsh reaction conditions make it an urgent priority to develop a convenient and mild method.

Mussel adhesive proteins excreted by marine mussels have the abilities of strong adhesion and secondary reaction for multifunctional coatings. A facile surface modification approach inspired by the adhesion mechanism of mussels was introduced by Lee et al. In this approach, the self-polymerization of dopamine produced an adherent poly(dopamine) (PDA) as the functional layer on various substrates, including organic and inorganic materials.[27−30] The results indicate that dopamine and other catechol compounds perform well as binding agents for metal ions and reducing agents for reducing metal ions to elemental metals.[31,32] This method is versatile for its simple ingredients, mild reaction conditions, and applicability to various materials with complex shapes. The PDA could be readily used to immobilize adherent and uniform metal coating by electroless plating.

In this work, we used tetraethyl orthosilicate as a starting material to prepare inorganic SiNFs via the sol−gel electrospinning method followed by pyrolysis. The electrospun SiNF surface was then modified by self-polymerization of polydopamine and electroless plating of silver using glucose as a reducing agent. Resistivity is the most important part of conductive and EMI shielding applications, and it can be well controlled in this method. To demonstrate the conductive performance application of SiNFs-PDA/Ag, the electrical and

Received: January 14, 2014
Accepted: March 4, 2014
Published: March 20, 2014

   dx.doi.org/10.1021/am5002663 | ACS Appl. Mater. Interfaces 2014, 6, 5105−5112

mechanical properties of the silicon vulcanizate filled with SiNFs-PDA/Ag were studied in our work.

2. EXPERIMENTAL SECTION

2.1. Materials. Tetraethylorthosilicate (TEOS), polyvinylpyrrolidone (PVP, M_w = 1 300 000), dopamine·HCl, tris(hydroxymethyl)-aminomethane (Tris), and glucose were obtained from Alfa Aesar Company, U. S. A. Silver nitrate, ammonia, hydrochloric acid, ethanol, dimethyl sulfoxide (DMSO), and *N*,*N*-dimethylformamide (DMF) were purchased from Beijing Chemical Plant, China. All of the reagents and solvents were used as received and without further purification.

2.2. Preparation of SiNFs via Electrospinning. The spin dope was prepared by mixing the solution dissolved PVP (1.2 g) in DMF (5.0 g) and dimethyl sulfoxide (DMSO, 2.5 g) and the pregelation achieved by magnetic stirring of TEOS (3.2 g) with hydrochloric acid (37 wt %, 0.6 mL) and ethanol (0.9 mL) for 10 h in a vial under magnetic stirring for 3 h.

The spin dope was immediately filled into a plastic syringe with a blunt-tipped 22-gauge stainless-steel needle for electrospinning into the precursor nanofibers. A positive high voltage of 15 kV was applied to the needle with the high voltage power supply (ES30P) purchased from the Gamma High Voltage Research, Inc. (Ormond Beach, FL), and the feed rate of 1.0 mL/h was maintained with a KDS-200 syringe pump. The electrospun nanofibers were collected with an aluminum foil covered receiver that was electrically grounded and placed 10 in. from the tip of the needle. Due to the moisture in the atmosphere, the TEOS turned into gel completely by keeping the nanofiber mats under ambient conditions (temperature of 25 °C and relative humidity of 50%) for 48 h.

The electrospun precursor nanofibers were carefully peeled off from the aluminum foil and transferred in a crucible to a muffle oven to pyrolyze into the final SiNFs. The optimal pyrolysis procedure based upon fiber properties was heating at 350 °C for 3 h followed by heating at 800 °C for 6 h. The SiNFs were then naturally cooled off to room temperature.

2.3. Surface Modification of SiNFs by Polydopamine. The SiNFs were surface modified with aqueous solutions of dopamine·HCl at concentrations ranging from 0.5 to 4.0 g/L. The pH of each solution was buffered to 8.5 by adding Tris, which can form a Tris-HCl buffer solution with the HCl of dopamine·HCl. The solution pH was monitored with a pH meter (Mettler Toledo FE-20) fitted with a combined glass electrode (0.01 pH units). The solution was stirred for 24 h at room temperature, and the color of the solution changed from light pink to dark brown. The SiNFs coated with PDA were suction filtered, rinsed thoroughly with deionized water, and dried in a vacuum oven at 40 °C for 12 h. The PDA coated SiNFs will be denoted as SiNFs-PDA-x in the subsequent discussion, where x stands for the concentration of dopamine.

2.4. Electroless Deposition of Silver on the SiNFs-PDA Surface. The SiNFs-PDA were electroless plated in a silver plating bath prepared by dissolving silver nitrate (concentration varies from 1 to 20 g/L) into distilled water and adding ammonia slowly until the solutions became transparent again. Then SiNFs-PDA (concentration of 1 g/L) were added into the above solutions and kept magnetically stirring for 30 min. The same volume of glucose solution (at a concentration twice as high as that of silver nitrate) serving as a reducing agent was added slowly into the above mixture. The reduction was allowed to continue for 2 h under stirring at room temperature. The silver deposited SiNFs-PDA were suction filtrated, washed 3 times with distilled water, and dried in a vacuum oven at 40 °C for 6 h. The obtained samples will be denoted as SiNFs-PDA/Ag-y, where y stands for the concentration of silver nitrate.

2.5. Characterization. X-ray photoelectron spectroscopy (XPS) measurements were carried out on an ESCALAB 250 XPS system (Thermo Electron Corporation, USA) with an Al Kα X-ray source (1486.6 eV photons). The core-level signals were obtained at a photoelectron takeoff angle of 45° with respect to the sample surface. The X-ray source was run at a reduced power of 150 W. The powdered samples were pressed into tablets and mounted on standard sample studs by means of double-sided adhesive tapes. The pressure in the analysis chamber was maintained at 10−8 Torr or lower during each measurement. To compensate for surface charging effects, all binding energies (BEs) were referenced to the C 1s hydrocarbon peak at 284.6 eV.

Scanning electron microscopy (SEM) was performed on a Hitachi S-4700 scanning electron microscope (Hitachi, Japan). The surface of the samples was sputtered with a thin layer of gold before the measurements. The SEM measurements were accomplished at accelerating voltages of 5 kV and 20 kV.

Transmission electron microscopy (TEM) images were recorded on an FEI TAICNAI G^2 20 STWIN transmission electron microscope at an accelerating voltage of 200 kV, and energy dispersive spectrometry (EDS) was performed on an EDAX GENESIS XM 30rT energy dispersive X-ray spectrometer attached to the transmission electron microscope. The specimens of electrospun precursor nanofibers for TEM observations were prepared by receiving the nanofibers with the carbon support films during the electrospinning process. Other specimens were prepared by dropping sample suspensions onto carbon support films, and the solvent was allowed to evaporate before observation.

X-ray diffraction (XRD) patterns of the samples were recorded on a Bruker D8 Advance (Germany). The testing voltage was 40 kV. The current was 40 mA. The scan speed was 0.1 s/step, and the diffraction patterns were recorded in the 2θ range of 5°−90°.

Thermogravimetric analysis (TGA) was performed on a STARe system from 30 to 800 °C at a heating rate of 10 °C/min with a steady nitrogen flow (50 mL/min).

The electrical resistivity of the samples was measured with a four-point probe (Keithley 2400 source measure unit with a semiautomatic wafer probe with tungsten tips to make contacts, Guangzhou, China). The spacing between the tips was 0.05 in., and the radius of the tip was 0.004 in. Before each measurement, the silverized SiNFs were pressed into 1 mm sheets by using a tablet press with a maximum pressure of 10 MPa.

3. RESULTS AND DISCUSSION

3.1. Preparation of SiNFs via Electrospinning. The chemical composition of the electrospun precursor nanofibers (PNFs) was analyzed with EDS. The atomic percentages of C, O, and Si are 14.90%, 58.78%, and 26.22%, respectively. The presence of carbon in SiNFs is due to the carbon in PVP. The atomic ratio of O to Si is 2.24, which is higher than the theoretical value in SiO_2 because PVP contains oxygen as well.

The surface morphology of SiNFs obtained by the pyrolysis of PNFs was investigated with SEM. The SEM image (Figure 1) shows that the average diameter of SiNFs is about 300 nm, and the surface of SiNFs is quite smooth. Different spin dope

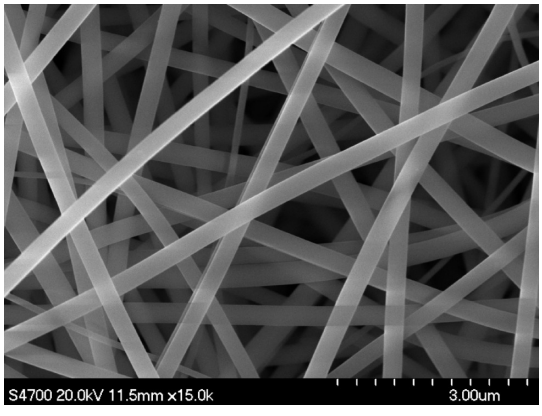

Figure 1. SEM image of electrospun silica nanofibers.

Scheme 1. Schematic Illustration of Processes for Preparation of SiNFs-PDA/Ag by Dopamine Functionalization and Electroless Silver Plating

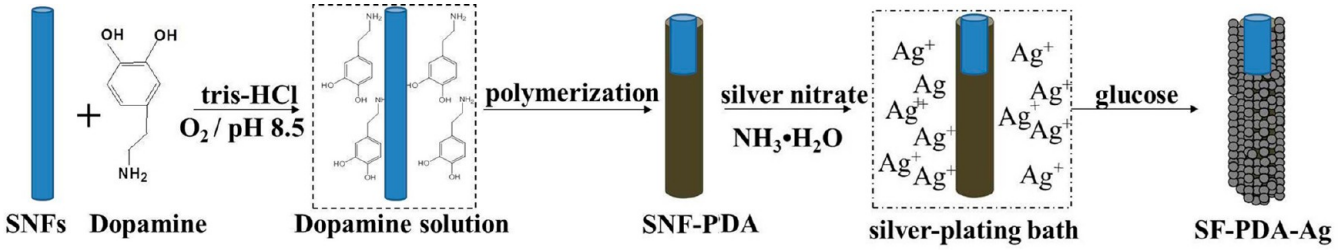

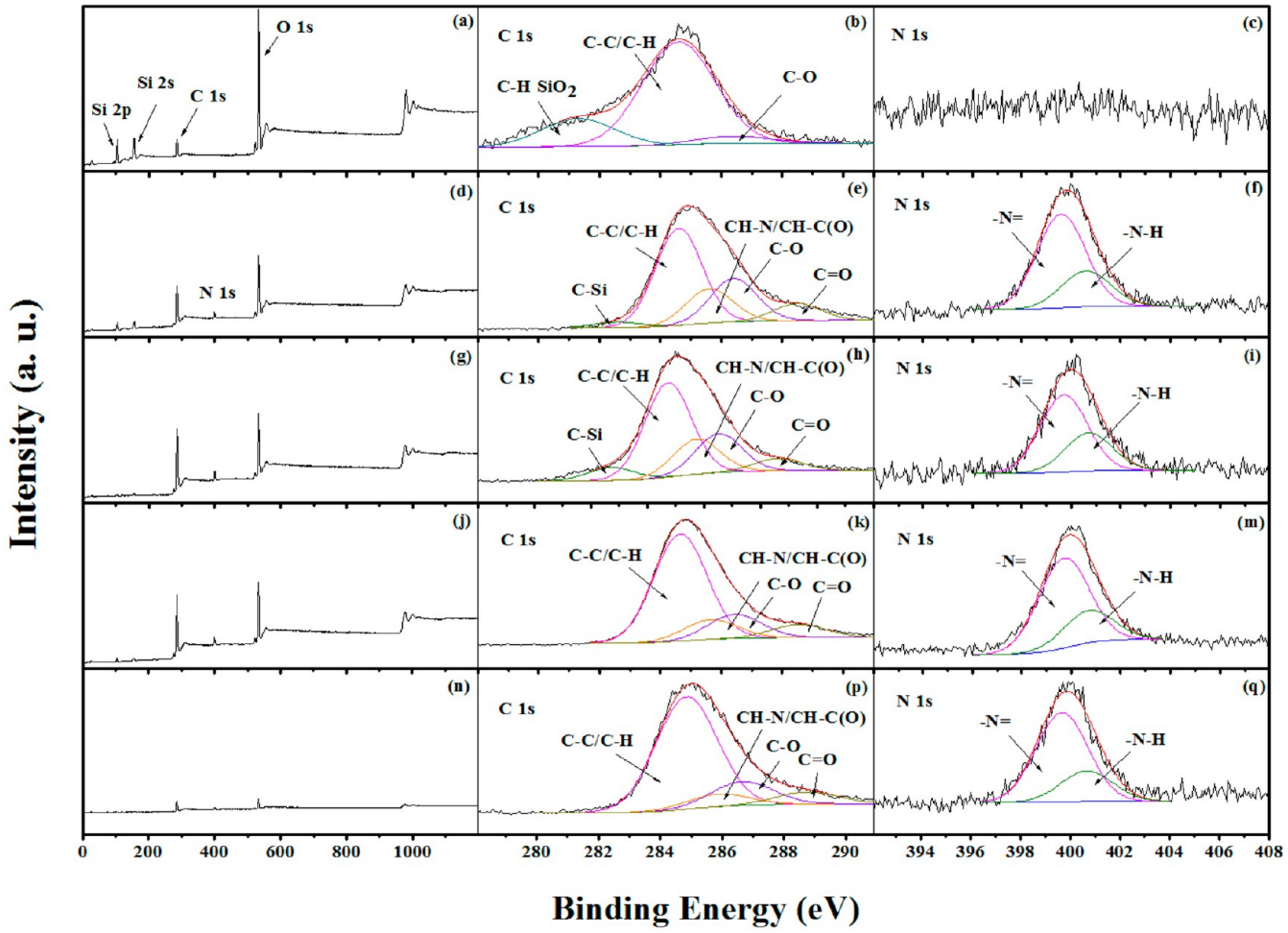

Figure 2. XPS spectra of (a, d, g, j, n) wide scan spectra, (b, e, h, k, p) C 1s core-level spectra, and (c, f, i, m, q) N 1s core-level spectra of SiNFs, SiNF-PDA-0.5, SiNF-PDA-2, SiNF-PDA-4, and PDA homopolymer.

formulas were studied, and the relationship between the diameter of SiNFs and the concentration of PVP was developed. The diameter of SiNFs can be controlled between 100 and 500 nm, and consequently different diameters of SiNFs-PDA/Ag can be prepared on demand.

3.2. Modification of SiNFs by Polydopamine (the SiNFs-PDA Surface). The process of dopamine self-polymerization on the surface of SiNFs is shown in Scheme 1. The mechanism for the in situ spontaneous oxidative polymerization of dopamine is elusive now. The interaction between PDA and inert substrates is probably intermolecular force since it is difficult to form covalent bonds between PDA and inert surfaces.

The chemical compositions of the surfaces of SiNFs and SiNFs-PDA were determined by XPS. Figure 2 shows the XPS spectra of the as-prepared products: a, d, g, j, and n, wide scan spectra; b, e, h, k, and p, C 1s core-level spectra; and c, f, i, m, and q, N 1s core-level spectra of SiNFs, SiNF-PDA-0.5, SiNF-PDA-2, SiNF-PDA-4, and PDA homopolymer, respectively. The XPS wide scan of the SiNFs shows four major peaks, which are 105 eV for the Si 2p, 156 eV for the Si 2s, 285 eV for the C 1s, and 534 eV for the O 1s peak. The XPS wide scan spectra of SiNFs-PDA show the appearance of a new peak component at the binding energy (BE) of about 400 eV, which is attributed to the nitrogen-containing species in PDA. The presence of PDA on the SiNF surface can also be deduced from the decrease of O 1s peak intensity and the increase of C 1s peak intensity as a

dx.doi.org/10.1021/am5002663 | ACS Appl. Mater. Interfaces 2014, 6, 5105−5112

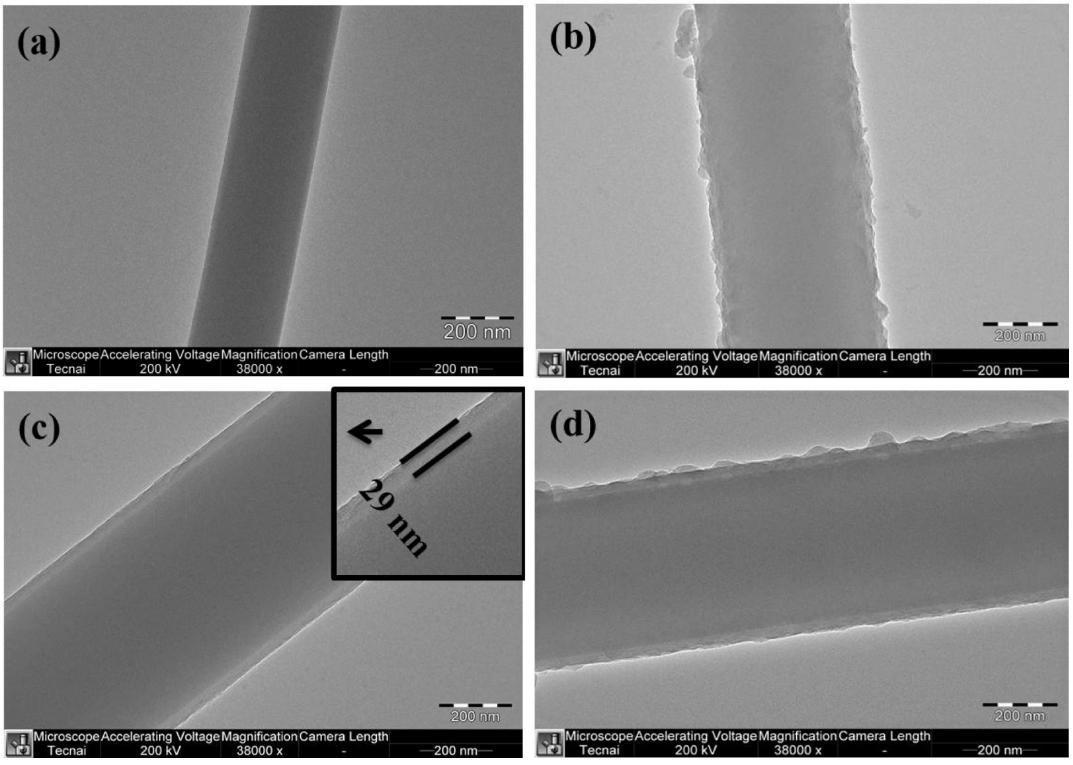

Figure 3. The TEM images of (a) SiNF, (b) SiNF-PDA-0.5, (c) SiNF-PDA-2, and (d) SiNF-PDA-4.

result of the lower oxygen content of PDA. As there is no carbon in the SiNFs, the small C 1s peak is attributed to the surface absorption of the SiNFs. The distinction between the peak intensity of SiNFs-PDA-0.5 and that of SiNFs-PDA-2 is obvious, while the peak intensities of higher dopamine concentrations looks similar, which can be interpreted as the thickness of the deposited PDA being over the probing depth of the XPS technique.[33] The C 1s core-level spectra of SiNFs-PDA-0.5 and SiNFs-PDA-2 can each be curve-fitted into five peak components at BEs of about 282.6, 284.6, 285.6, 286.4, and 288.5 eV, attributable to the C−Si, C−C, CH−N, C−O, and C═O species, respectively. The peak component for C−Si is due to the interaction between PDA and the SiNFs surface, and others are consistent with the PDA molecular structure. There is no C−Si peak component in the C 1s core-level spectrum of SiNF-PDA-4, probably because the thickness of the PDA layer was over the probing depth. The deposition of PDA on the surface of SiNFs is further verified by the N 1s core-level spectra of SiNFs-PDA. The N 1s spectra of SiNFs-PDA can be curve-fitted into two typical peaks at BEs of about 398.5 and 399.5 eV, attributable to the imine (═N−) and amine (−N−H) species, respectively. On the basis of the conjectural polymerization mechanism of PDA, the ═N− species is attributed to the structure evolution during the self-polymerization of dopamine, while the −N−H species is formed through the amine group of the dopamine. The above results confirm the in situ spontaneous oxidative polymerization of dopamine on the SiNF surface.

TEM was used to observe the morphologies of SiNFs and SiNFs-PDA. The TEM images of SiNFs (Figure 3a), SiNFs-PDA-0.5 (Figure 3b), SiNFs-PDA-2 (Figure 3c), and SiNFs-PDA-4 (Figure 3d) are shown in Figure 3. A pristine SiNF has a smooth surface, while a SiNF-PDA is coated with a uniform PDA layer whose thickness is controllable. With the increase of the dopamine concentration, the thickness of the PDA layer increases and the surface smoothness increases, but with further increases in concentration to 4g/L or higher, the surface smoothness of SiNFs-PDA decreases. The thickness of the PDA layer is about 29 nm at a dopamine concentration of 2 g/L.

TGA was used to confirm the successful polymerization of dopamine and determine the amount of PDA on the SiNF surface. The TGA curves of SiNFs and SiNFs-PDA prepared at different dopamine concentrations were shown in Figure 4. As the samples are heated to 800 °C, SiNFs show a weight loss of 3.8%, and pure PDA obtained by the in situ oxidative polymerization of 2.0 g/L of dopamine shows a weight loss

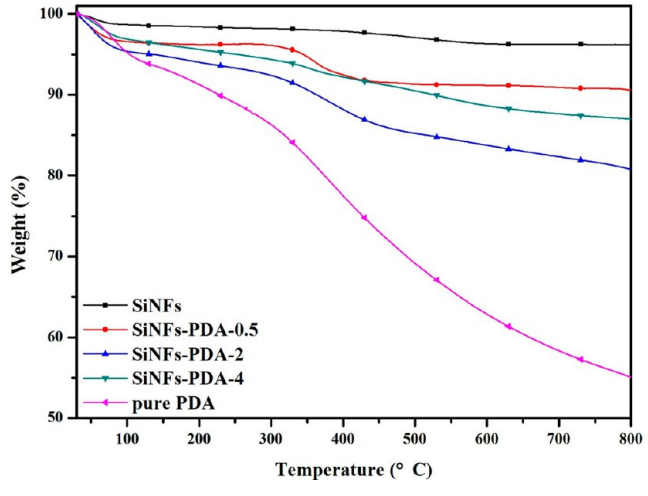

Figure 4. TGA thermograms of SiNFs and SiNFs-PDA prepared with different dopamine concentrations.

dx.doi.org/10.1021/am5002663 | ACS Appl. Mater. Interfaces 2014, 6, 5105−5112

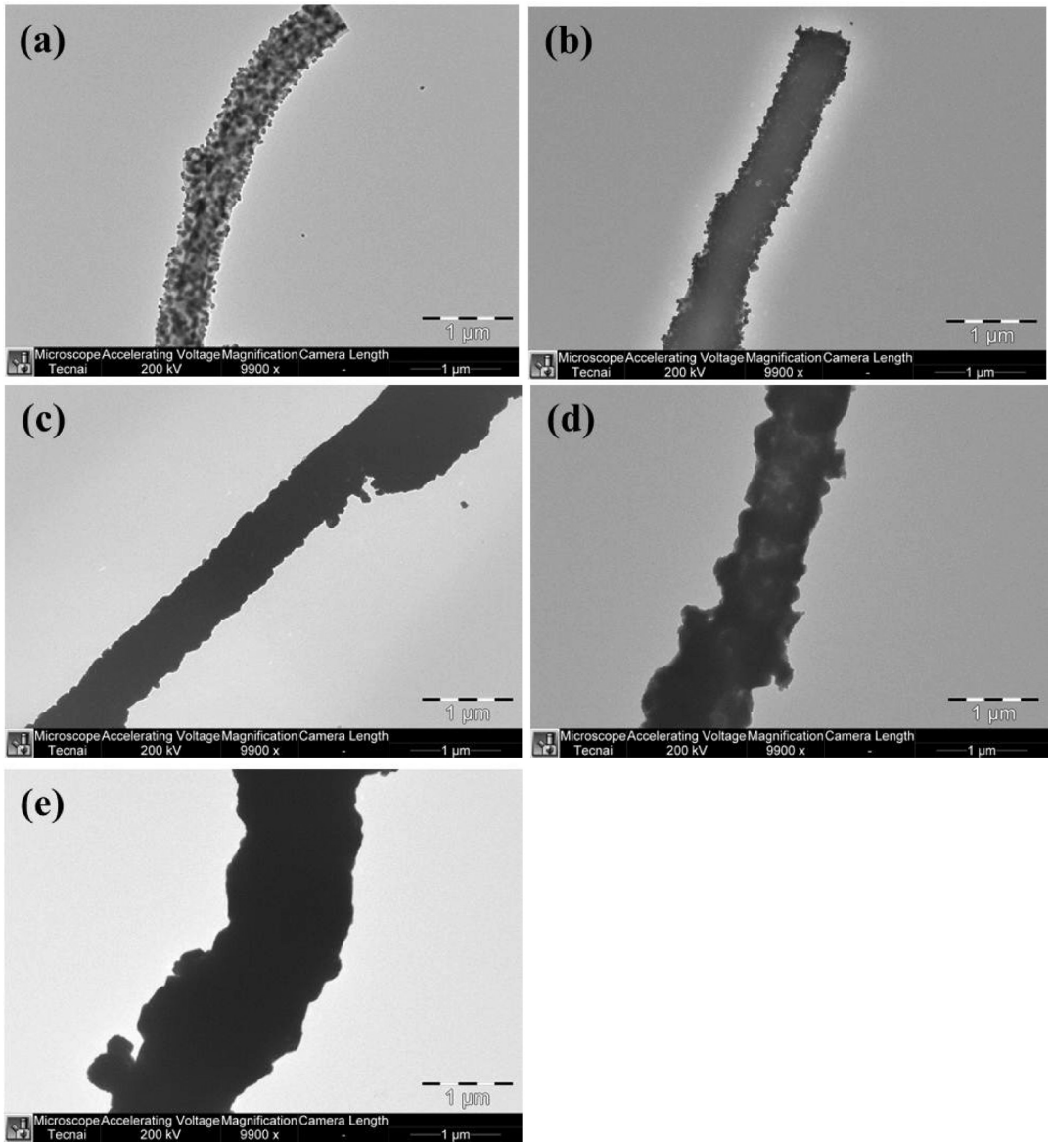

Figure 5. TEM images of SiNFs-PDA/Ag prepared with different $AgNO_3$ concentrations: (a) SiNFs-PDA/Ag-1, (b) SiNFs-PDA/Ag-3, (c) SiNFs-PDA/Ag-5, (d) SiNFs-PDA/Ag-10, and (e) SiNFs-PDA/Ag-20.

of 44.9%. Thus, from the weight losses of SiNFs-PDA-0.5, SiNFs-PDA-2, and SiNFs-PDA-4 of 9.5%, 19.2%, and 13.0%, it can be calculated that the PDA contents of SiNFs-PDA-0.5, SiNFs-PDA-2, and SiNFs-PDA-4 are about 13.7%, 37.5%, and 22.4%, respectively. These results indicate that the thickness and amount of the PDA coating layer first increases and then decreases with the concentration of dopamine increasing, in accordance with the TEM results.

3.3. Electroless Deposition of Silver on SiNF-PDA Surface. The process of electroless deposition of silver on the SiNF-PDA surface is shown in Scheme 1. The metal-binding ability of catechol and nitrogen-containing groups present in the PDA structure was exploited to immobilize silver nanoparticles onto the SiNF-PDA surface. The $[Ag(NH_3)_2]^+$ ions adsorbed by catechol and nitrogen-containing groups could be reduced into silver nanoparticles by a reducing agent.[18] SiNFs-PDA-2 was selected to prepare SiNFs-PDA/Ag hybrids for its smooth surface and the moderate PDA layer thickness.

The micromorphology of SiNF-PDA/Ag was observed by TEM. The TEM images of SiNFs-PDA/Ag-1 (Figure 5a) and SiNFs-PDA/Ag-3 (Figure 5b) show that uniformly dispersed discrete silver clusters assembled on the SiNFs-PDA surface but did not form a continuous silver layer. With increasing $AgNO_3$ concentration, more silver particles aggregated on the SiNF surface, leading to the formation of a continuous, uniform, and compact silver layer on the SiNF-PDA surface, as can be seen from the TEM images of SiNFs-PDA/Ag-5 (Figure 5c), SiNFs-PDA/Ag-10 (Figure 5d), and SiNFs-PDA/Ag-20 (Figure 5e). On the other hand, however, the surface of SiNFs-PDA/Ag prepared with excessively high $AgNO_3$ concentrations is uneven and loose because the crystal growth was too fast at high concentrations of silver ions and reducing agent. The chemical composition of SiNFs was investigated with EDS simultaneously, and the results are given in Figure 6, which shows that the silver content of SiNFs-PDA/Ag increases with the increasing of $AgNO_3$ concentration. The silver content of SiNFs-PDA/Ag is about 49.8% with the concentration of

dx.doi.org/10.1021/am5002663 | ACS Appl. Mater. Interfaces 2014, 6, 5105−5112

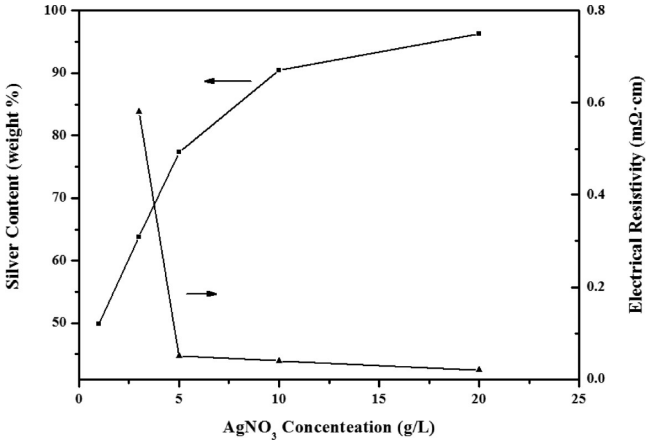

Figure 6. Silver content and electrical resistivity versus $AgNO_3$ concentration for SiNFs-PDA/Ag.

$AgNO_3$ of 1 g/L, and the silver content of SiNFs-PDA/Ag reaches about 96.5% when the concentration of $AgNO_3$ is 20 g/L. Too high $AgNO_3$ concentrations lead to excessively high silver contents, which bring about nothing but resource-wasting and excessive cost. Hence, the optimum concentration of $AgNO_3$ is 5 g/L.

The crystalline structures of SiNFs were determined by XRD. Figure 7 shows the diffraction patterns of SiNFs (Figure 7a),

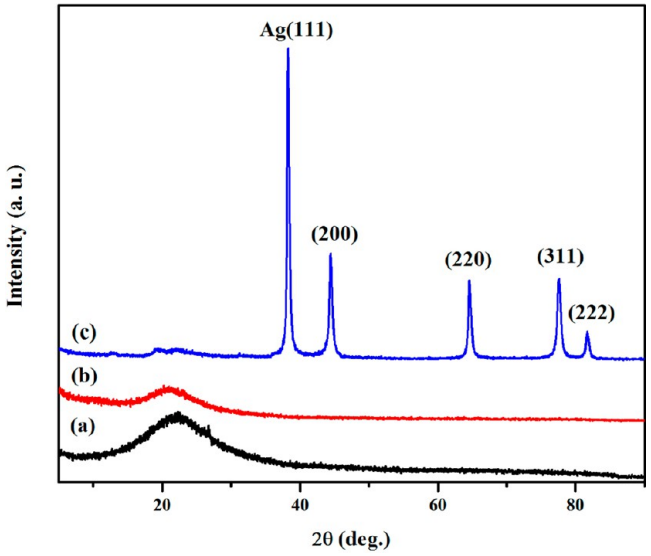

Figure 7. Diffraction patterns of (a) SiNFs, (b) SiNFs-PDA, and (c) SiNFs-PDA/Ag.

SiNFs-PDA (Figure 7b), and SiNFs-PDA/Ag (Figure 7c). It can be seen from Figure 7a and b that the typical amorphous peak of silica appears in the pattern of SiNFs, and this peak of silica does not change in the pattern of SiNFs-PDA, an indication that PDA does not affect the amorphous structure of SiNFs. The SiNFs-PDA/Ag diffraction pattern (Figure 7c) shows five sharp diffraction peaks at 38.2, 44.2, 64.4, 78.4, and 81.6°, corresponding to the Ag (111), Ag (200), Ag (220), Ag (311), and Ag (222) planes, respectively. This diffraction pattern of SiNFs-PDA/Ag matches exactly with the standard pattern of silver (JCPDS, no. 04-0783), indicating the successful reduction of Ag^+ to Ag^0 by using glucose as a reducing agent in the presence of PDA, consistent with the presence of Ag indicated by EDS measurements.

The electrical resistivity of SiNFs-PDA/Ag fabricated with different $AgNO_3$ concentrations is shown in Figure 6. As shown in Figure 5a, the silver particles electrolessly plated on SiNFs-PDA/Ag at a $AgNO_3$ concentration of 1 g/L are individual and discrete, resulting in a nonconductive surface and an electrical resistivity that is not measurable. The electrical resistivity reaches 0.58 mΩ·cm at the $AgNO_3$ concentration of 3 g/L; however, a further increase of the $AgNO_3$ concentration to 5 g/L significantly reduces the electrical resistivity to about 0.05 mΩ·cm (high conductivity). The decrease in electrical resistivity indicates that the silver particles reduced on the SiNF surface form a continuous and compact silver coating, which is consistent with the increase in silver content with increasing $AgNO_3$ concentration. But increasing the $AgNO_3$ concentration to above 5 g/L does not reduce the electrical resistivity of SiNFs-PDA/Ag markedly as the electrical resistivity to 0.02 mΩ·cm at the $AgNO_3$ concentration of 20 g/L (shown in Figure 6), a further illustration that the optimum concentration of $AgNO_3$ is 5 g/L. The ability of the shielding effectiveness at various frequencies is determined by the resistivity of this material that depends on the continuity and thickness of the silver layer. Additionally, in theory, the percolation threshold of nanofiller composites is much lower than that of the microfiller composites commonly used now. The lower percolation threshold results from conjunct effects of dispersion, a conductive network, and nanoeffect.[34,35]

3.4. Conductive Silicon Elastomer Filled by SiNFs-PDA/Ag. To further study the electrical conductivity of the as-prepared nanofibers, silicon rubber filled with the SiNFs-PDA/Ag was prepared by using a two-roll mill. The rubber was then vulcanized in a compression molding press at 175 °C. Some mechanical properties and the electrical resistivity of the vulcanized silicon rubber filled with SiNFs-PDA/Ag are shown in Table 1. The tensile strength and hardness (shore A)

Table 1. Mechanical Behavior and Electrical Property of the Silicon Rubber Composites

samples	Ts/MPa	Eb/%	Ts at 100%/MPa	hardness (shore A)	electrical resistivity/Ω·cm
0 phr	2.07	275.51	0.64	32	
15 phr	2.74	288.75	1.01	45	0.58
60 phr	3.22	154.82	2.12	50	0.05
100 phr	3.28	158.72	2.40	55	0.04

increase with increasing filler content. The tensile strength of the silicon rubber without filler was 2.07 MPa, and the hardness was 32, while the tensile strength was 3.28 MPa, and the hardness was 55 at 100 phr, which is due to the reinforcement of short fibers. The electrical resistivity of the silicon vulcanized rubber decreases from 8.1×10^{12} Ω·cm to 0.079 Ω·cm with increasing filler content from 0 phr to 100 phr. The good electrical property makes the SiNFs-PDA/Ag-filled silicon rubber a conductive elastomer, and with an electrical resistivity much lower than 10 Ω·cm, this filled rubber can be used as an electromagnetic shielding elastomer.

The morphology of the SiNFs-PDA/Ag before (Figure 8a) and after (Figure 8b) blending with silicon rubber was observed by SEM. The SiNFs-PDA/Ag after blending was separated from the silicon rubber compound by dissolving the compound in *n*-hexane, filtered, and dried. The average length of SiNFs-

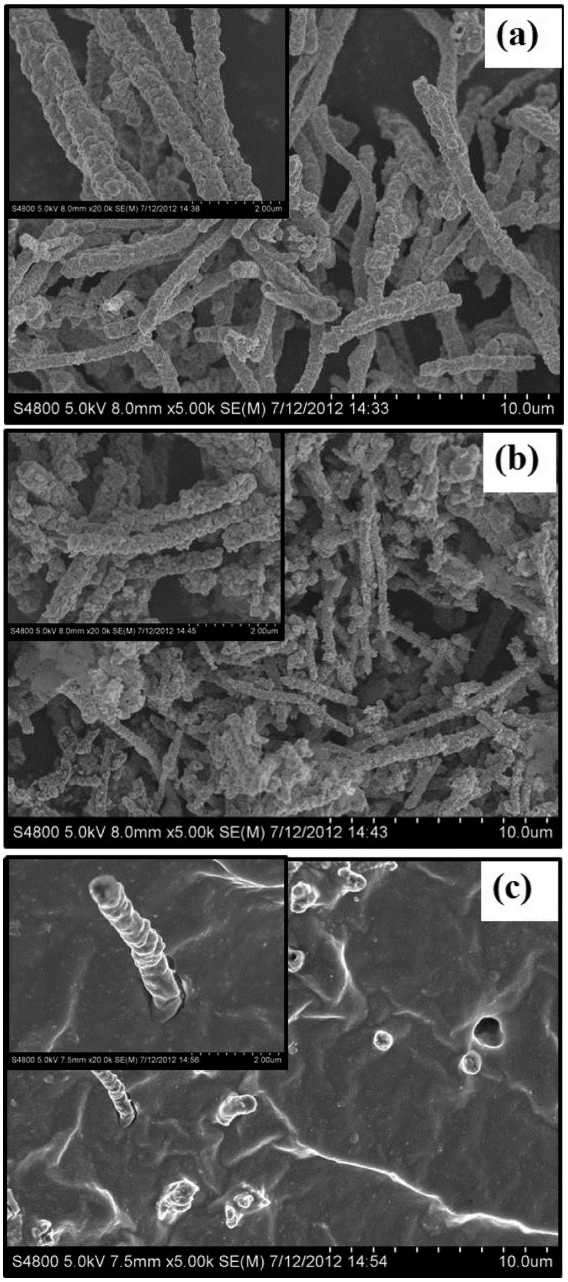

Figure 8. SEM images of (a) SiNFs-PDA/Ag before blending, (b) SiNFs-PDA/Ag after blending with silicon rubber, and (c) tensile fractured surfaces of the silicon vulcanized rubber filled with SiNFs-PDA/Ag.

PDA/Ag decreased after blending because of the shear force during the blending. However, the absence of crushed fibers indicates that the strength of SiNFs-PDA/Ag is quite high. The silver layer remains continuous and compact after blending, demonstrating the strong interaction between the silver layer and the SiNFs-PDA. The tensile fractured surfaces of the silicon vulcanized rubber filled with SiNFs-PDA/Ag were also observed by SEM. The SEM image is shown in Figure 8c, from which we can see the pulled-out fibers and the holes left behind after the pull-out. The silver shell of the pulled-out fibers remains intact, further indicating the high strength of SiNFs-PDA/Ag and the strong adhesion of the silver layer to SiNFs-PDA.

4. CONCLUSION

A simple approach to prepare highly conductive one-dimensional nanocomposite by electroless plating of Ag NPs on the surface of electrospun SiNFs via the polydopamine functionalization was studied. Randomly distributed Ag NPs with controllable density were deposited on the surface of SiNFs-PDA due to the polydopamine layer with catechol and amine functional groups, which can be used as the chemisorption sites for silver ions and the adhesion promotion layer for Ag NPs. A continuous and highly homogeneous colloidal silver shell can be achieved on the surface of SiNFs-PDA. The resultant silver uptake on the SiNF-PDA surface is strongly dependent on the concentration of the metal salt solution. The as-prepared SiNFs-PDA/Ag show high conductivity, and the bonding between the silver layer and SiNFs-PDA is strong. The high conductivity and strong bonding make SiNFs-PDA/Ag promising as conductive composites for a broad range of applications.

AUTHOR INFORMATION

Corresponding Author

*Tel.: +86-10-64434860. Fax: +86-10-64433964. E-mail: wangw@mail.buct.edu.cn.

Notes

The authors declare no competing financial interest.

ACKNOWLEDGMENTS

The authors sincerely appreciate the financial supports from the Natural Science Foundation of China (Grant No. 51373010, 51221002), the Program for New Century Excellent Talents in University (NCET-11-0562), and the Natural Science Foundation of Beijing City (No. 2122049).

REFERENCES

(1) Ye, W.; Hu, H.; Zhang, H.; Zhou, F.; Liu, W. Multi-walled Carbon Nanotube Supported Pd and Pt Nanoparticles with High Solution Affinity for Effective Electrocatalysis. *Appl. Surf. Sci.* **2010**, *256*, 6723−6728.

(2) Sureshkumar, M.; Siswanto, D.; Lee, C. Magnetic Antimicrobial Nanocomposite Based on Bacterial Cellulose and Silver Nanoparticles. *J. Mater. Chem.* **2010**, *20*, 6948−6955.

(3) Gottlieb, D.; Morin, S.; Jin, S.; Raines, R. Self-Assembled Collagen-like Peptide Fibers as Templates for Metallic Nanowires. *J. Mater. Chem.* **2008**, *18*, 3865−3870.

(4) Guo, S.; Dong, S.; Wang, E. Constructing Carbon Nanotube/Pt Nanoparticle Hybrids Using an Imidazolium-salt-based Ionic Liquid as a Linker. *Adv. Mater.* **2010**, *22*, 1269−1272.

(5) Kotál, V.; Švorčík, V.; Slepička, P.; Sajdl, P.; Bláhová, O.; Šutta, P.; Hnatowicz, V. Gold Coating of Poly(ethylene terephthalate) Modified by Argon Plasma. *Plasma Process. Polym.* **2007**, *4*, 69−76.

(6) Greiner, A.; Wendorff, J. Electrospinning: a Fascinating Method for the Preparation of Ultrathin Fibers. *Angew. Chem., Int. Ed. Engl.* **2007**, *46*, 5670−5703.

(7) Li, D.; McCann, J.; Xia, Y.; Marquez, M. Electrospinning: a Simple and Versatile Technique for Producing Ceramic Nanofibers and Nanotubes. *J. Am. Ceram. Soc.* **2006**, *89*, 1861−1869.

(8) Wen, S.; Liu, L.; Zhang, L.; Chen, Q.; Zhang, L.; Fong, H. Hierarchical Electrospun SiO_2 Nanofibers Containing SiO_2 Nanoparticles with Controllable Surface-roughness and/or Porosity. *Mater. Lett.* **2010**, *64*, 1517−1520.

(9) Choi, S.; Lee, G.; Im, S.; Kim, H.; Joo, L. Silica Nanofibers from Electrospinning/Sol-gel Process. *J. Mater. Sci. Lett.* **2003**, *22*, 891−893.

(10) Shao, C.; Kim, H.; Gong, J.; Lee, D. A Novel Method for Making Silica Nanofibres by Using Electrospun Fibres of Poly-

vinylalcohol/Silica Composite as Precursor. *Nanotechnology* **2002**, *13*, 635−637.
(11) Patel, A.; Li, S.; Wang, C.; Zhang, W.; Wei, Y. Electrospinning of Porous Silica Nanofibers Containing Silver Nanoparticles for Catalytic Applications. *Chem. Mater.* **2007**, *19*, 1231−1238.
(12) Zhang, S.; Ni, W.; Kou, X.; Yeung, M.; Sun, L.; Wang, J.; Yan, C. Formation of Gold and Silver Nanoparticle Arrays and Thin Shells on Mesostructured Silica Nanofibers. *Adv. Funct. Mater.* **2007**, *17*, 3258−3266.
(13) Huang, W.; Chen, H.; Zuo, J. One-dimensional Self-assembly of Metallic Nanostructures on Single-walled Carbon-nanotube Bundles. *Small* **2006**, *2*, 1418−1421.
(14) Lyandres, O.; Yuen, J.; Shah, N.; VanDuyne, R.; Walsh, J., Jr.; Glucksberg, M. R. Progress toward an in vivo Surface-enhanced Raman Spectroscopy Glucose Sensor. *Diabetes Technol. Ther.* **2008**, *10*, 257−265.
(15) Liao, Y.; Wang, Y.; Feng, X.; Wang, W.; Xu, F.; Zhang, L. Antibacterial Surfaces through Dopamine Functionalization and Silver Nanoparticle Immobilization. *Mater. Chem. Phys.* **2010**, *121*, 534−540.
(16) Sureshkumar, M.; Lee, P.; Lee, C. Stepwise Assembly of Multimetallic Nanoparticles via Self-Polymerized Polydopamine. *J. Mater. Chem.* **2011**, *21*, 12316−12320.
(17) Moon, J.; Kim, K.; Choi, H.; Lee, S.; Park, S. Electroless Silver Coating of Rod-like Glass Particles. *Ultramicroscopy* **2008**, *108*, 1307−1310.
(18) Xu, C.; Tian, M.; Liu, L.; Zou, H.; Zhang, L.; Wang, W. Fabrication and Properties of Silverized Glass Fiber by Dopamine Functionalization and Electroless Plating. *J. Electrochem. Soc.* **2012**, *159*, D217−D224.
(19) Wang, W.; Cheng, W.; Tian, M.; Zou, H.; Li, L.; Zhang, L. Preparation of PET/Ag Hybrid Fibers via a Biomimetic Surface Functionalization Method. *Electrochim. Acta* **2012**, *79*, 37−49.
(20) Tang, Z.; Kotov, N. One-Dimensional Assemblies of Nanoparticles: Preparation, Properties, and Promise. *Adv. Mater.* **2005**, *17*, 951−962.
(21) Qu, W.; Bao, H.; Zhang, L.; Chen, G. Far-infrared-assisted Preparation of a Graphene-nickel Nanoparticle Hybrid for the Enrichment of Proteins and Peptides. *Chem.—Eur. J.* **2012**, *18*, 15746−15752.
(22) Lin, W.; Xi, X.; Yu, C. Research of Silver Plating Nano-graphite Filled Conductive Adhesive. *Synth. Met.* **2009**, *159*, 619−624.
(23) Wei, H.; Eilers, H. Electrical Conductivity of Thin-film Composites Containing Silver Nanoparticles Embedded in a Dielectric Fluoropolymer Matrix. *Thin Solid Films* **2008**, *517*, 575−581.
(24) Lu, Y.; Jiang, S.; Huang, Y. Ultrasonic-assisted Electroless Deposition of Ag on PET Fabric with Low Silver Content for EMI Shielding. *Surf. Coat. Technol.* **2010**, *204*, 2829−2833.
(25) Zhang, Z.; Shao, C.; Zou, P.; Zhang, P.; Zhang, M.; Mu, J.; Guo, Z.; Li, X.; Wang, C.; Liu, Y. In situ Assembly of Well-dispersed Gold Nanoparticles on Electrospun Silica Nanotubes for Catalytic Reduction of 4-nitrophenol. *Chem. Commun.* **2011**, *47*, 3906−3908.
(26) Zhang, Z.; Shao, C.; Sun, Y.; Mu, J.; Zhang, M.; Zhang, P.; Guo, Z.; Liang, P.; Wang, C.; Liu, Y. Tubular Nanocomposite Catalysts Based on Size-controlled and Highly Dispersed Silver Nanoparticles Assembled on Electrospun Silica Nanotubes for Catalytic Reduction of 4-nitrophenol. *J. Mater. Chem.* **2012**, *22*, 1387−1395.
(27) Lee, H.; Dellatore, S.; Miller, W.; Messersmith, P. Mussel-inspired Surface Chemistry for Multifunctional Coatings. *Science* **2007**, *318*, 426−430.
(28) Lee, H.; Lee, B.; Messersmith, P. A Reversible Wet/Dry Adhesive Inspired by Mussels and Geckos. *Nature* **2007**, *448*, 338−341.
(29) Lee, Y.; Lee, H.; Kim, Y.; Kim, J.; Hyeon, T.; Park, H.; Messersmith, P.; Park, T. Bioinspired Surface Immobilization of Hyaluronic Acid on Monodisperse Magnetite Nanocrystals for Targeted Cancer Imaging. *Adv. Mater.* **2008**, *20*, 4154−4157.
(30) Postma, A.; Yan, Y.; Wang, Y.; Zelikin, A.; Tjipto, E.; Caruso, F. Self-polymerization of Dopamine as a Versatile and Robust Technique to Prepare Polymer Capsules. *Chem. Mater.* **2009**, *21*, 3042−3044.
(31) Messersmith, P. Multitasking in Tissues and Materials. *Science* **2008**, *319*, 1767.
(32) Fei, B.; Qian, B.; Yang, Z.; Wang, R.; Liu, W.; Mak, C.; Xin, J. Coating Carbon Nanotubes by Spontaneous Oxidative Polymerization of Dopamine. *Carbon* **2008**, *46*, 1795−1797.
(33) Wang, W.; Vora, R.; Kang, E.; Neoh, K. Electroless Plating of Copper on Fluorinated Polyimide Films Modified by Surface Graft Copolymerization with 1-vinylimidazole and 4-vinylpyridine. *Polym. Eng. Sci.* **2004**, *44*, 362−375.
(34) Bauhofer, W.; Kovacs, J. A review and Analysis of Electrical Percolation in Carbon Nanotube Polymer Composites. *Compos. Sci. Technol.* **2009**, *69*, 1486−1498.
(35) Dalmas, F.; Cavaillé, J.; Gauthier, C.; Chazeau, L.; Dendievel, R. Viscoelastic Behavior and Electrical Properties of Flexible Nanofiber Filled Polymer Nanocomposites. Influence of Processing Conditions. *Compos. Sci. Technol.* **2007**, *67*, 829−839.